PSEUDO-THREE DIMENSIONAL THERORETICAL PREDICTION OF LOCAL TEMPERATURE IN AN INTERIOR PERMANENT MAGNET MOTOR USING A LUMPED PARAMETER HEAT TRANSFER MODEL

Lee J.H.[1], Lee N.K[1], Choi M.S[2] and Um S.K.[1]*
*Author for correspondence
[1]Department of Mechanical Engineering, Hanyang University, Seoul, 133-791, South Korea,
[2]Higen Motor Co., LTD., Changwon, 51555, South Korea,
E-mail: jonghyolee@hanyang.ac.kr

ABSTRACT

Interior permanent magnet (IPM) motors have been receiving much attention as special drive applications for industrial robots, servomechanisms, and electric vehicles because of their low cost and high efficiency. In general, magnets in IPM motors show the highest temperatures, particularly under high speed operating conditions, causing durability problems in motor performance. The purpose of this study was twofold. One goal is to propose effective thermal network modeling of circular electric motors by using a lumped-parameter network method, which is based on an axisymmetric motor structure. For this purpose, a pseudo-three dimensional thermal network model (TNM) is developed to reflect periodical repetitions of coil and yoke in the angular direction. The other is to conduct effective thermal analysis by manipulating key design and operating variables. As a validation process of the TNM model, temperatures at representative motor components were compared under the same operating conditions. Both theoretical and numerical results by the TNM and three dimensional computation results show minor temperature differences less than 5% in all parts of the motor. In subsequent applications, the TNM was utilized to predict maximum coil and magnet temperatures, derive heat transfer paths, and estimate heat losses through various directions of the motor. The TNM enables us to predict the heat distribution in various types of motors and derive optimized geometrical parameters in a convenient way.

INTRODUCTION

The interior permanent magnet (IPM) motor has been widely used in various applications such as industrial robots, electric vehicles and servomechanisms due to its high efficiency, high power density and compact size [1]. However, in high speed operating condition, the energy losses at coil and core may result high temperature. In general, high temperature cause the component durability problems in motors. Therefore, it is important to predict exact thermal distribution use thermal analysis in electric motors under various driving [2].

Numerous researches have focused on thermal analysis of electrical motors. For thermal analysis of electrical motors computational fluid dynamics (CFD) and lumped-parameter network methods are widely utilized [3]. The CFD are generally used to model and analyse the heat transfer within complex structures of electric motors. Maynes and Aldo compared numerical models with experiment results by CFD, and Chang et al. applied various cooling method to analysis the thermal characteristics of motor [4]. Huang et al. conducted similar studies to acquire a reliable time-dependent heat flux by using CFD. It had a better correct analysis but requires more difficult modeling process and longer calculation time.

The lumped-parameter network models are consisted of thermal resistances, capacitances, and power losses analysis. The lumped-parameter network models are suitable for the thermal model of electric motor and has apparent advantages on simplicity and timesaving. Yaman and Daniel presented lumped-parameter thermal model that made by thermal resistance and introduced thermal network modeling method. Ilhan et al. created a thermal equivalent circuit (TEC) model to analysis for the steady-state and transient thermal performance of the flux switching permanent magnet (FSPM) motor [5]-[6]. Bellettre et al. applied, among the listed method, the nodal method, because it is suitable for transient and proposed model.

The objective of this study is to predict thermal path using the thermal network model (TNM) using lumped-parameter network method. However, it is difficult to predict and analyse the temperature of motors in various operating condition, particularly of rotating speed and geometric variable. The Nusselt number and Taylor number is applied in this study for advanced thermal model. In addition, the thermal network is based on geometric variable for thermal resistances and an easy control.

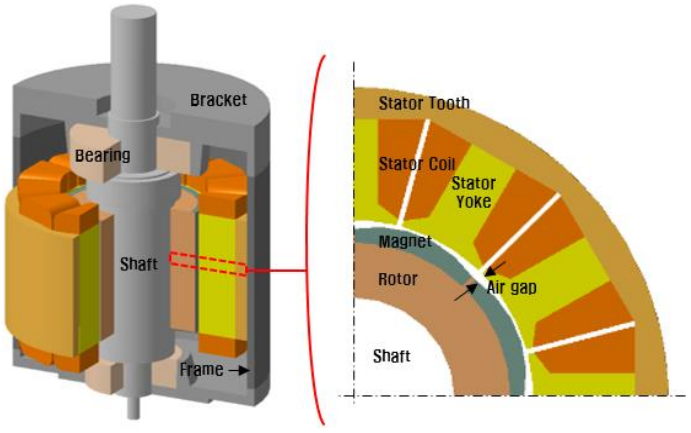

Figure 1 The major component of IPM motor

Table 1 Operating conditions of a reference model

Quantity	Value
Motor type	IPM Motor
Output power	1.3 kW
Rated speed	1,500 rpm
Total losses	170.45 W
Cooling type	Air-cooling
Convection	15 W/m^{2}K

THEORETICAL MODELING

In this study, the IPM motor with a driving speed of 1,500 rpm was defined as a reference model. More detailed operating condition of the reference model are show in Table 1. Total losses from electric motors are separated into three groups as copper loss, core loss and mechanical loss. In general, mechanical losses are considered negligible because it occur less than 3% of the total loss. This study is assumed that the core losses only appear in stator and magnet.

Thermal Resistances

A reference model is axisymmetric organization shown in Figure 1. Conduction through cylindrical structure can be determined from the radius. The relationship of resistances between two components is shown in Figure 2 [7]-[8]. The thermal resistance for heat transfer is defined as follows:

$$R_1 = \frac{\ln(r_c / r_i)}{2\pi kL} \quad (1)$$

$$R_2 = \frac{\ln(r_o / r_c)}{2\pi kL} \quad (2)$$

$$R_{3,4} = \frac{L/2}{2\pi k(r_o^2 - r_i^2)} \quad (3)$$

where k is the thermal conductivity of the material, r is radius of the components and L is height of the surface area. $T_{m,n}$ represent the temperature of a node in components. Total thermal resistances in a node is the sum of that resistances each direction.

$$R_{total} = R_1 + R_2 + R_3 + R_4 \quad (4)$$

The thermal paths and distribution can be calculated using thermal resistances. The thermal model is composed thermal network using thermal resistances.

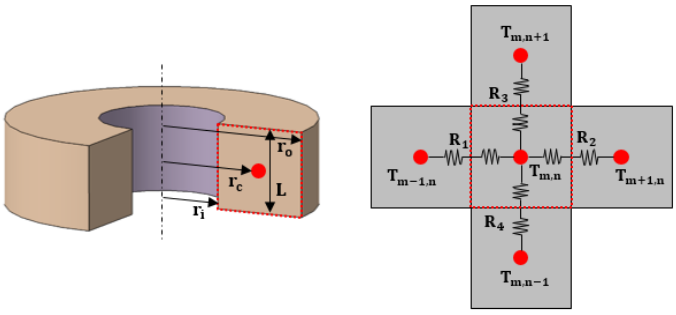

Figure 2 Thermal resistances of axisymmetric components

Thermal Network

TNM in this study is a pseudo-3D theoretical network model. This network structure is based on axisymmetric models and simple composition of thermal resistance. Due to the complication of the IPM motor, the thermal network required a simple composition of thermal resistance. Although TNM is composed pseudo-3D, the stator parts was applied 3D direction using arithmetic mean. The stator parts are divided into three categories: stator coil, stator core, air gap. Here the air gap is not space that between rotor and stator. They have different volume rates that stator coils are 51%, stator cores are 44% and air gaps are 5%. The heat easily passes through components with higher thermal conductivity. Therefore, stator parts are assumed as a single part using the arithmetic mean. Then the effective thermal conductivity of stator parts can be calculated using the formulation:

$$k_{total} = \frac{k_1 a + k_2 b}{(a+b)} = f_1 k_1 + f_2 k_2 \quad (2)$$

where k_{total} represent the total thermal conductivity of a single part. k_1 and k_2 are the thermal conductivities of the volumes a and b. f is the volume fraction. The overall thermal network is formed resistances of nodes shown in Figure 4.

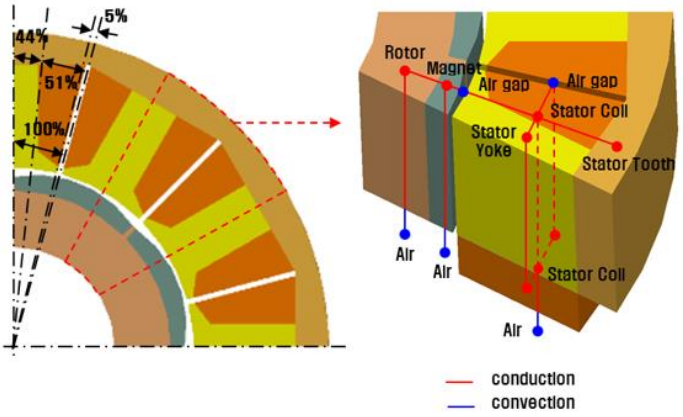

Figure 3 Volume rate and thermal network in stator parts

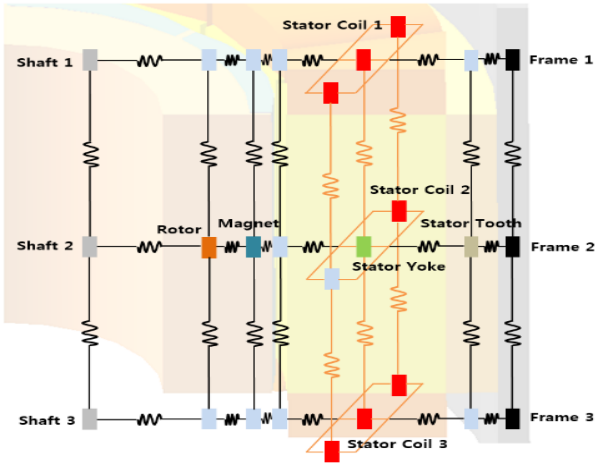

Figure 4 The Pseudo-3D thermal network of motor

Modeling of Air gap Region

The heat transfer in fluid depends on characteristics of the flow. When the fluid moves quickly, it is generally considered a conductive material. Particularly, the nature of flow in the air gap is determined by Taylor number and Nusselt number [9]-[10]. Because, the operating state of motor is a similar Taylor-Couette flow. Reynold number and Taylor number can be calculated from:

$$\mathrm{Re} = \frac{\Omega r d}{v} \tag{5}$$

$$Ta = \frac{\Omega^2 r d^3}{v^2} \tag{6}$$

where Ω is angular velocity, r is radius of rotor, d is length of the air gap and v is the kinematic viscosity of the air. Nusselt number can be expressed as follows:

$$Nu = 2 \tag{7}$$

$$Nu = 0.409 Ta^{0.241} - 137 Ta^{-0.75} \tag{8}$$

Nusselt number is 2 in an area smaller than 1,740. The effective thermal conductivity can be expressed as follows:

$$k_{airgap}^{eff} = Nu \times k_{air} \tag{9}$$

If the boundary condition due to rotation under operating conditions is smaller than the air gap, heat transfer does not occur. Because, the air gap is divided into an insulating region and a boundary layer. Heat transfer can occur at boundary layer, but the heat transfer does not occur well because the stationary region has a low value of heat transfer coefficient. The boundary layer can be calculated from:

$$\delta = \frac{4.91 l}{\mathrm{Re}^{1/2}} \tag{10}$$

$$\delta = \frac{0.38 l}{\mathrm{Re}^{1/5}} \tag{11}$$

where δ is boundary layer, l is fluid length and Re is Reynold number.

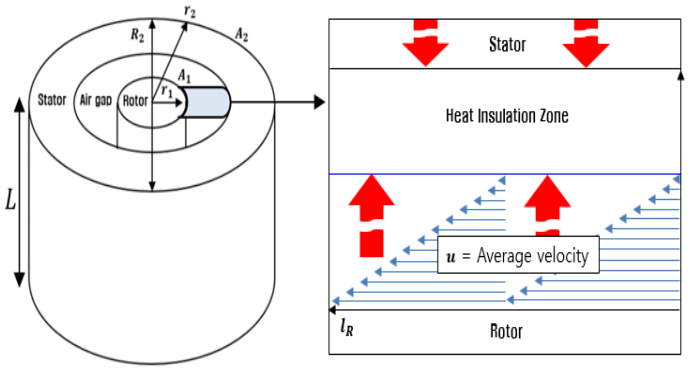

Figure 5 fluid flow and boundary layer in air gap

RESULTS AND DISCUSSION

Due to identify reliability of the theoretical model, the reference electric motor was analyzed through experiments, CFD and theoretical analysis.

Numerical Analysis

The model assumed incompressible, negligible contact resistance, uniform heat flux and natural convection. Generally operations of motor is described by mass, momentum, energy principles. In study, flow characteristic of CFD model was analyzed using moving rotation frame (MRF) method. MRF has various advantages that reduction of working time and suitable for rotating model. Analysis ranges of MRF are divided fixed region and rotating region shown Figure 6. The fixed regions in Figure 6 can be expressed as follows:

$$\nabla \cdot (\overline{u_i} \otimes \overline{u_i}) = -\nabla \frac{P}{\rho} + v \nabla^2 \overline{u_i} \tag{12}$$

The rotating regions can be expressed as follows:

$$\nabla \cdot (\overline{u_r} \otimes \overline{u_r})\bar{r} + 2\overline{\omega} \times \overline{u_r} + \overline{\omega} \times \overline{\omega} \times \bar{r} = -\nabla \frac{P}{\rho} + v \nabla^2 \overline{u_r} \tag{13}$$

where $\bar{r}$ is position vector in rotating frame, $\overline{\omega}$ is angular velocity of rotating frame, $\overline{u_r}$ is relative velocity and $\overline{u_t}$ is absolute velocity.

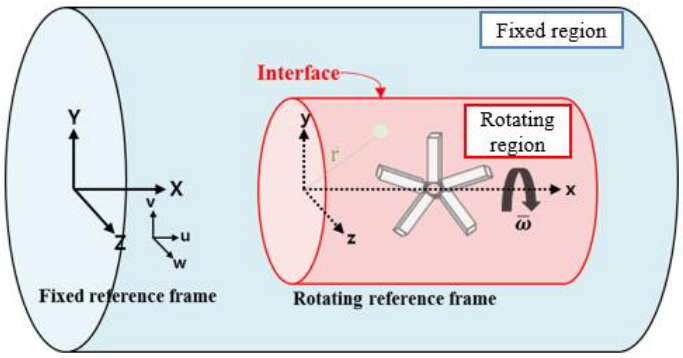

Figure 6 Analysis ranges of MRF method

Table 2 and Figure 7 shows thermal analysis results in the analysis models with the same operating condition. Results show that the reliability of TNM had high. The theoretical thermal results have a low error of less than 1%. However, an error of plate part have high value. The shape of plate in TNM depends on axisymmetric, but in the experiment it is a cuboid. Besides, it can display the thermal distribution in diagram form. We found that the similar results in same region as shown in Figure 8.

Table 2 thermal analysis results

	Experiment	CFD	TNM
Stator Coil	357.3 K	357.4 K	359.4 K
Magnet	-	349.7 K	351.4 K

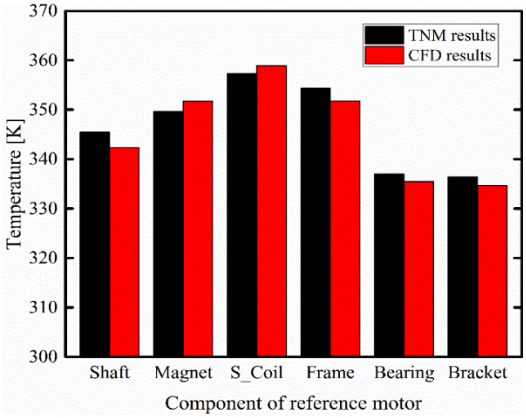

Figure 7 The maximum temperature of components

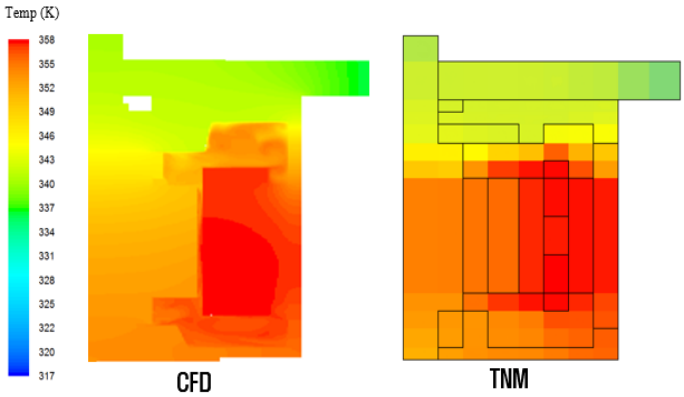

Figure 8 Thermal distribution in a reference model

Thermal Path of TNM

In this study, a value of input losses is identical to a value of output losses. Because, the total heat losses of motors is lost to ambient by air-cooling. The heat losses at located components by outside are presented in Table 3. Figure 9 and Table 3 display that the large amount of heat is lost by plate. It should be noticed that the rate of heat losses was decided by the size of contact surface. The heat transfer rate can be expressed as follows:

$$Q_{cond} = kA\frac{\Delta T}{l} \tag{14}$$

$$Q_{conv} = hA\Delta T \tag{15}$$

Under the identical heat transfer coefficient, heat generates are increased if the contact surface is increase. The plate has high heat losses, but the shaft has low heat losses. Because, the contact surface of the shaft is smaller than the plate.

Geometric Variable

The TNM has variable tools such as geometric value, the heat loss, rotation speed and thermal resistance. So, the various thermal analyses were performed using TNM. Figure 10 shows the maximum temperature of stator coil due to plate contact surface changes. When the contact surface is 100%, the maximum temperature of the reference model is 359.4 K. However, when the contact surface is half, the maximum temperature increases from 359.4K to 366.7K in the stator coil. Because, under the identical heat generate, the temperature difference increases if the contact surface is reduce. Figure 11 shows the changes of temperature with frame thickness variation. The reference thickness of frame is 0.004 m. When it is increase, the temperature is reduce. As the thickness increases, the thermal resistance and surface also increases. However, the thermal resistance from frame to bracket decreases. Because, the contact surface of bracket and frame is increase.

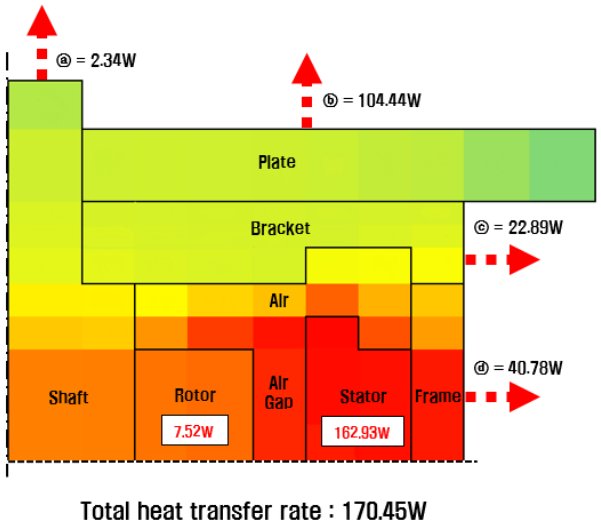

Figure 9 Composition of components and thermal path

Table 3 The values of heat losses in the motor

	Plate	Frame	Bracket	Shaft	Total
Loss	104.44 W	40.78 W	22.89 W	2.34 W	170.45 W
Rate	61.3 %	23.9 %	13.4 %	1.4 %	100 %

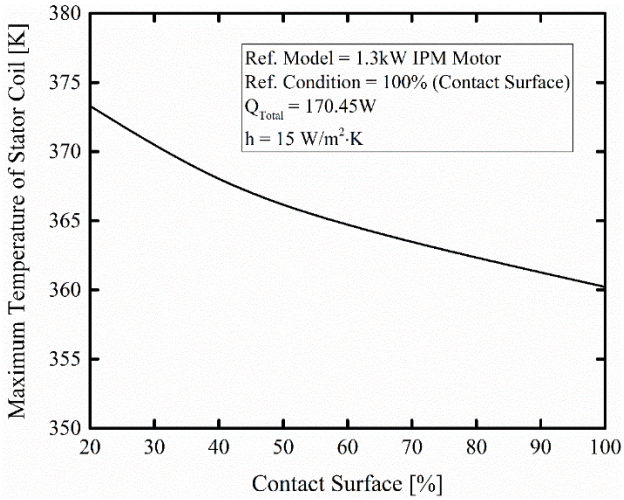

Figure 10 Maximum temperatures of stator coil

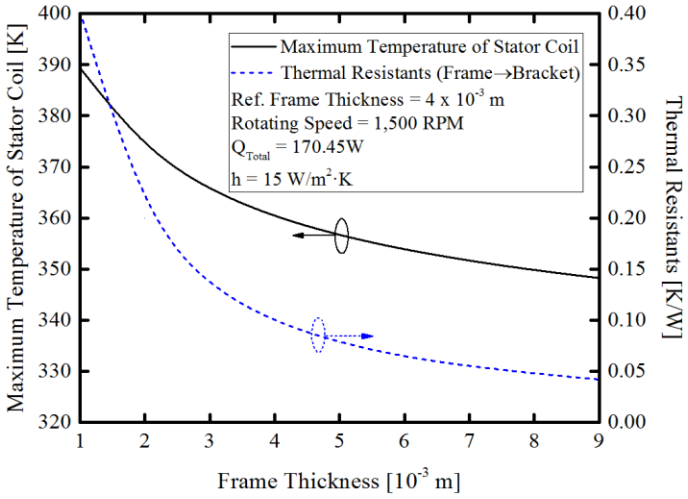

Figure 11 Maximum temperature and thermal resistance

CONCLUSION

The TNM based lumped-parameter network method was proposed to prediction the thermal path for the thermal analysis results of this study shows good agreement with the CFD thermal analysis results. The thermal resistance was changed for cylindrical structure due to motors are based on axisymmetric. The stator parts are assumed as a single part by using the arithmetic mean of the effective conductivity. The Nusselt number and Taylor number were applied to the air gap for rotation effect. In this study, the thermal analysis results shows the importance of the thermal resistances. The thermal path and loss tend to depend on the thermal resistances. When the contact surface and length are increase, the temperature of motors was decrease due to the thermal resistances were increase.

ACKNOWLEDGEMENTS

This research was supported by the Ministry of Trade, Industry & Energy (MOTIE), Korea Evaluation Institute of Industrial Technology in Republic of Korea. (Project No. 10051147 & No. 10063006)

REFERENCES

[1] Demetriades G. D., Parra H. Z., Andersson E., and Olsson H., A real-time thermal model of a permanent-magnet synchronous motor, *IEEE Transactions on Power Electronics*, Vol. 25, No. 2, 2010, pp. 463-474

[2] Dajaku G., and Gerling D., An improved lumped parameter thermal model for electrical machines, *17th International Conference on Electrical Machines (ICEM)*, 2006

[3] Chin Y. K., and Staton D. A., Transient thermal analysis using both lumped-circuit approach and finite element method of a permanent magnet traction motor, *7th AFRICON Conference in Africa*, Vol. 2, 2004, pp. 1027-1036

[4] Boglietti A., Cavagnino A., Lazzari M., and Pastorelli M., A simplified thermal model for variable-speed self-cooled industrial induction motor, *IEEE Transactions on Industry Applications*, Vol. 39, No. 4, 2003, pp. 945-952

[5] Ilhan E., Kremers M. F. J., Motoasca T. E., Paulides J. J. H., and Lomonova E., Transient thermal analysis of flux switching PM machines, *2013 Eighth International Conference and Exhibition on Ecological Vehicles and Renewable Energies*, 2013, pp. 1-7

[6] Kolondzovski Z., Belahcen A., and Arkkio A., Multiphysics thermal design of a high-speed permanent-magnet machine, *Applied Thermal Engineering*, Vol. 29, No. 13, 2009, pp. 2693-2700

[7] Junak J., Ombach G., and Staton D., Permanent magnet DC motor brush transient thermal analysis, *Proceeding of the 2008 International Conference on Electrical Machines*, No. 1109, 2008, pp. 978-1

[8] Staton D., Boglietti A., and Cavagnino A., Solving the more difficult aspects of electric motor thermal analysis in small and medium size industrial induction motors, *IEEE Transactions on Energy Conversion*, Vol. 20, No. 3, 2005, pp. 620-628

[9] Taylor, G. I, Stability of a viscous liquid contained between two rotating cylinders, *Philosophical Transactions of the Royal Society of London*, No. 223, 1923, pp. 289-343

[10] Mellor P. H., Roberts D., and Turner D. R., Lumped parameter thermal model for electrical machines of TEFC design, *IEE Proceedings B-Electric Power Applications*, Vol. 138, No. 5, 1991, pp. 205-218